*Inorg. Chem.* **2008**, *47*, 1753−1764


# Forum

## Mechanisms of Water Oxidation Catalyzed by Ruthenium Diimine Complexes

**James K. Hurst,* Jonathan L. Cape, Aurora E. Clark, Samir Das, and Changyong Qin**

*Department of Chemistry, Washington State University, Pullman, Washington 99164-4630*

Received April 16, 2007

$^{18}O$-isotope-labeling studies have led to the conclusion that there exist two major pathways for water oxidation catalyzed by dimeric ruthenium ions of the general type *cis,cis*-$[L_2Ru^{III}(OH_2)]_2O^{4+}$. We have proposed that both pathways involve concerted addition of H and OH fragments derived from $H_2O$ to the complexes in their four-electron-oxidized states, i.e., $[L_2Ru^{V}(O)]_2O^{4+}$, ultimately generating bound peroxy intermediates that decay with the evolution of $O_2$. The pathways differ primarily in the site of addition of the OH fragment, which is either a ruthenyl O atom or a bipyridine ligand. In the former case, water addition is thought to give rise to a critical intermediate whose structure is $L_2Ru^{IV}(OH)ORu^{IV}(OOH)L_2^{4+}$; the structures of intermediates involved in the other pathway are less well defined but may involve bipyridine OH adducts of the type $L_2Ru^{V}(O)ORu^{IV}(OH)(L^{\bullet}OH)L^{4+}$, which could react further to generate unstable dioxetanes or similar endoperoxides. Published experimental and theoretical support for these pathways is reviewed within the broader context of water oxidation catalysis and related reactions reported for other diruthenium and group 8 monomeric diimine-based catalysts. New experiments that are designed to probe the issue of bipyridine ligand "noninnocence" in catalysis are described. Specifically, the relative contributions of the two pathways have been shown to correlate with substituent effects in 4,4′- and 5,5′-substituted bipyridine complexes in a manner consistent with the formation of a reactive OH-adduct intermediate in one of the pathways, and the formation of OH-bipyridine adducts during catalytic turnover has been directly confirmed by optical spectroscopy. Finally, a photosensitized system for catalyzed water oxidation has been developed that allows assessment of the catalytic efficiencies of the complex ions under neutral and alkaline conditions; these studies show that the ions are far better catalysts than had previously been assumed based upon reported catalytic parameters obtained with strong oxidants in acidic media.

### Introduction

Early research on water oxidation catalyzed by transition-metal complex ions was focused primarily on alkaline decay reactions of group 8 $M(bpy)_3^{3+}$ reactions (reviewed in ref 1), which gave rise to detectable $O_2$ among a number of decomposition products.[2] Important observations emanating from that body of work are that spectroscopic signatures were identified that indicate the formation of intermediary species formed by OH addition to the bipyridine rings[3] and that irreversible degradation of the $M(bpy)_3^{3+}$ ions could be largely averted by blocking bimolecular reactions via zeolite encapsulation[4] or the addition of other redox ions, e.g., $Co^{2+}$, which presumably functioned as electron donors and alternative water oxidation catalysts.[5] These latter discoveries have led to the development of several fairly efficient photocatalytic cycles based upon $Ru(bpy)_3^{3+}$-photosensitized reactions between sacrificial electron acceptors and a variety of ions, metal complexes, and metal oxides.[1,6]

Our interest in water oxidation began ∼20 years ago, during which time one of us (J.K.H.) participated in collaborative studies with Michael Grätzel's group at EPFL-

* To whom correspondence should be addressed. E-mail: hurst@wsu.edu. Phone: 509-335-7848. 509-335-8867.

(1) Hurst, J. K. *Coord. Chem. Rev.* **2005**, *249*, 313.
(2) Ghosh, P. K.; Brunschwig, B. S.; Chou, M.; Creutz, C.; Sutin, N. *J. Am. Chem. Soc.* **1984**, *106*, 4772.
(3) Creutz, C.; Sutin, N. *Proc. Natl. Acad. Sci. U.S.A.* **1975**, *72*, 2858.
(4) Ledney, M.; Dutta, P. *J. Am. Chem. Soc.* **1995**, *117*, 7687.
(5) Brunschwig, B. S.; Chou, M. H.; Creutz, C.; Ghosh, P.; Sutin, N. *J. Am. Chem. Soc.* **1983**, *105*, 4832.

10.1021/ic700724h CCC: $40.75 
Published on Web 03/10/2008

Lausanne on reactions catalyzed by dimeric $\mu$-oxo-bridged ruthenium complex ions of the class *cis*,*cis*-$[L_2Ru^{III}(OH_2)]_2O^{4+}$, where L is 2,2′-bipyridine or a ring-substituted congener. The capacity of these "blue" dimers to catalyze water oxidation, discovered within the group of Meyer[7] and subsequently reproduced in several other laboratories,[8–11] represented the first (and, for many years, the only) verified class of coordination complex ions capable of sustained catalysis of water oxidation. This capability was evident from direct measurement of the $O_2$ evolution in acidic media containing strong oxidants ($Ce^{4+}$ and $Co^{3+}$)[7–10] and in photosensitized reactions in media containing a sacrificial electron acceptor ($S_2O_8^{2-}$)[9] and from voltammetric experiments that indicated a ~100–200 mV decrease in measured overpotentials for breakdown of the aqueous solvent when the catalyst was present.[9,11,12] These observations engendered considerable initial enthusiasm among chemists engaged in solar photoconversion research because it is widely believed that water is the only source of electrons capable of driving economically competitive photoproduction of $H_2$ as a large-scale alternative energy source; furthermore, coordination complexes are potentially advantageous as synthetically versatile and highly adaptive components for integrated photochemical systems capable of water splitting.

However, progress in understanding the underlying reaction mechanisms of these complexes since their initial discovery can be described most charitably as modest.

Numerous factors have contributed to difficulties in studying these reactions, ranging from their synthetic intractability[13] to the inability to isolate and physically characterize solutions of the ions in various accessible oxidation states. For example, although the optical absorption spectra of the complexes in their lowest stable oxidation states ({**3,3**})[14] are clearly distinguishable from the spectra of more highly oxidized species, those of the remaining states are very similar (Figure 1), rendering attempts at monitoring reaction dynamics by conventional spectroscopic methods extremely challenging. This problem is exacerbated by the redox properties of the dimers. Specifically, the circumstance

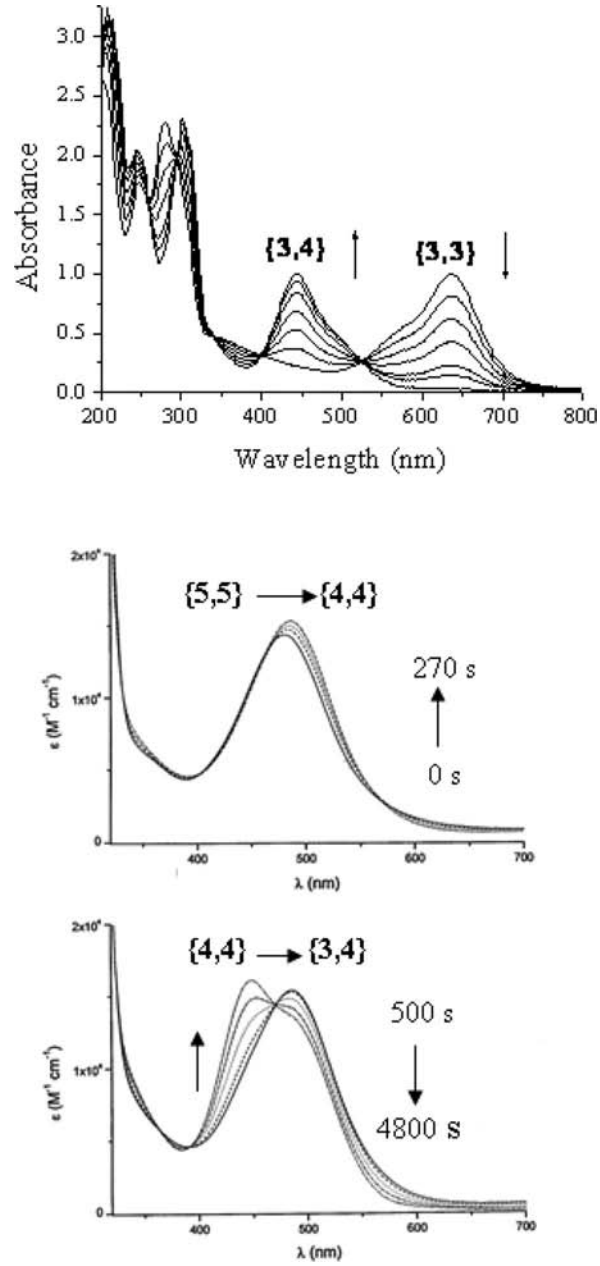


**Figure 1.** Optical spectra of {**3,3**}, {**3,4**}, {**4,4**}, and {**5,5**} in 0.5 M triflic acid. Upper panel: titration of {**3,3**} with 1 equiv of $Ce^{4+}$. Middle panel: time course of decay of {**5,5**} → {**4,4**}. Lower panel: time course of decay of {**4,4**} → {**3,4**}. Note that the low-energy shoulder at 495 nm for {**3,4**} is the aquahydroxy complex ion, i.e., the conjugate base of the diaqua ion, which predominates in the weakly acidic region.[7]

that the reduction potentials for the functionally significant higher oxidation states are closely spaced and highly positive introduces considerable uncertainty in describing the actual composition of solutions prepared by chemical oxidation, especially when determined by optical spectroscopy. Cor-

(6) (a) Morris, N. D.; Suzuki, M.; Mallouk, T. E. *J. Phys. Chem. A* **2004**, *108*, 9115. (b) Kiwi, J.; Grätzel, M. *Angew. Chem., Int. Ed. Engl.* **1978**, *17*, 860. (c) Lehn, J. M.; Sauvage, J. P.; Ziessel, R. *Nouv. J. Chim.* **1980**, *4*, 355.

(7) Gilbert, J. A.; Eggleston, D. A.; Murphy, W. A., Jr.; Geselowitz, D. A.; Gersten, S. W.; Hodgson, D. J.; Meyer, T. J. *J. Am. Chem. Soc.* **1985**, *107*, 3855.

(8) Collin, J. P.; Sauvage, J. P. *Inorg. Chem.* **1986**, *25*, 135.

(9) Rotzinger, F. P.; Munavalli, S.; Comte, P.; Hurst, J. K.; Grätzel, M.; Pern, F.-J.; Frank, A. J. *J. Am. Chem. Soc.* **1987**, *109*, 6619.

(10) Hurst, J. K.; Zhou, J.; Lei, Y. *Inorg. Chem.* **1992**, *31*, 1010.

(11) Petach, H. H.; Elliott, C. M. *J. Electrochem. Soc.* **1992**, *139*, 2217.

(12) Comte, P.; Nazeruddin, M. K.; Rotzinger, F. P.; Frank, A. J.; Grätzel, M. *J. Mol. Catal.* **1989**, *52*, 63.

(13) Complexes formed from monomeric precursors whose bipyridine ligands bear weakly electron-donating substituents, such as 4,4′-dimethoxy-2,2′-bipyridine or 4,4′,5,5′-tetramethyl-2,2′-bipyridine, are prone to irreversible ligand oxidation and preferential formation of trimeric and higher oligomeric species, presumably via cis and trans geometrical isomerizations. Conversely, bipyridine ligands bearing moderately electron-withdrawing substituents, such as carboxy derivatives, form $\mu$-oxo dimers only under forcing conditions; to date, we have been unable to synthesize dimeric analogues whose bipyridine ligands contain more strongly electron-withdrawing substituents, such as nitro or trifluoromethyl groups.

(14) The notation in parentheses is used only to specify the overall oxidation state of the binuclear ion and, unless otherwise specified, is not intended to imply discrete oxidation states on the individual metal ions. For example, {**5,5**} represents an ion that contains four fewer electrons than {**3,3**}. Although {**5,5**} is formally written as $[(bpy)_2Ru^{V}(O)]_2O^{4+}$, recent DFT calculations suggest that the electron distribution for this ion is more appropriately represented by the chemical formula $[(bpy)_2Ru^{IV}(O^{\bullet})]_2O^{4+}$, i.e., a complex containing two terminal radicaloid oxo moieties.[15]

(15) Yang, X.; Baik, M.-H. *J. Am. Chem. Soc.* **2006**, *128*, 7476.

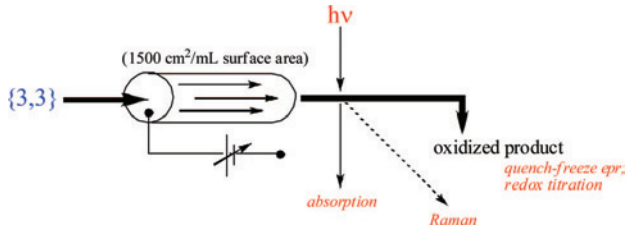


**Figure 2.** Schematic diagram of the flow electrolysis assembly for analysis of reactive oxidation states.

respondingly, much of our earlier research effort has been directed at developing alternative methods to prepare and physically characterize solutions to circumvent these technical problems. A particularly useful approach, at least for reactions in acidic solutions, has involved rapid constant potential electrolysis utilizing a commercial carbon fiber columnar flow electrode, which presents a very large surface area/volume ratio. When attached to a potentiostat, this cell allows one to control precisely the redox poise of reagent solutions, thereby providing access to a variety of kinetic and structural studies based upon electrochemical titrations (Figure 2).[16] As outlined in succeeding sections, the development in our laboratory of associated analytical methods based upon resonance Raman (RR) spectrophotometry, cryogenic electron paramagnetic resonance (EPR) spectrometry, and "real-time"mass spectrometry has greatly improved our understanding of the catalytic mechanisms.[17] Recent discoveries of additional classes of transition-metal complex ions capable of catalyzing water oxidation,[23–26] coupled with ongoing efforts to develop advanced computational methods to accurately model their physical properties and dynamical behavior,[15,27] should ultimately lead to identification of the underlying reactivity principles.

## Redox Properties and Reaction Pathways for *cis*,*cis*-$[L_2Ru^{III}(OH_2)]_2O^{4+}$ Ions

A typical RR spectroelectrochemical titration of the {**3,4**} ion in 0.5 M triflic acid is displayed in Figure 3.[16] Changes in the low-frequency RR spectra indicate sequential formation of two more highly oxidized complexes as the redox poise of the solution is raised. The intense Raman bands observed in the 360–390 $cm^{-1}$ region were identified as Ru−O−Ru symmetric stretching modes by $^{18}O$-isotope-induced shifts accompanying substitution at the bridging oxo ligand; similarly, the intense ∼820 $cm^{-1}$ band appearing in the most highly oxidized ion was identified as a Ru=O ruthenyl stretching mode by $^{18}OH_2$ substitution in the *cis*-aqua positions.[10,16,22,28] The possibility that the latter band arose from the formation of a bound peroxo ligand, whose O−O stretching frequency would be expected to lie in the same region, was excluded by examining the RR spectra in complexes containing ∼50% coordinated $^{18}OH_2$. Specifically, under these conditions, an O−O stretching mode would display three bands, corresponding to $^{16}O-^{16}O$, $^{16}O-^{16}O$, and $^{18}O-^{18}O$ isotopic distributions, whereas only two were observed, consistent with discrete Ru=$^{16}$O and Ru=$^{18}$O modes. Parallel optical spectrophotometric redox titrations using $Os(bpy)_3^{3+}$ to reduce the effluent solutions quantitatively to {**3,3**} established that the most highly oxidized species was {**5,5**}, i.e., a four-electron-oxidized species.[16] Meyer and co-workers have demonstrated the necessity for deprotonation of aqua ligands in achieving high formal oxidation states on transition-metal ions, which avoids accumulation of a positive electrostatic charge on the complex ions.[29,30] The appearance of the Ru=O ruthenyl stretching modes upon oxidation to {**5,5**} is consistent with this general principle; i.e., the overall oxidation reaction can be written as

$$[L_2Ru^{III}(OH_2)]_2O^{4+} \rightarrow [L_2Ru^{V}(O)]_2O^{4+} + 4[e^-] + 4H^+ \quad (1)$$

The oxidation state of the intermediary species is not currently agreed upon among researchers studying these complexes. On the basis of primarily their interpretation of cyclic voltammograms and rapid mixing spectrophotometry, Meyer and co-workers have suggested that the oxidation state is {**4,5**},[7,18,19] whereas our research is consistent only with

(16) Yamada, H.; Hurst, J. K. *J. Am. Chem. Soc.* **2000**, *122*, 5303.
(17) The catalysts are slowly irreversibly inactivated (by as-yet undetermined pathways) in solutions containing excess oxidant and can also undergo reversible anation at the *cis*-aqua positions to produce catalytically inactive complexes when appropriate ligands are present.[9] Mechanistic investigations by Meyer's group suggest that this anation can also occur during water oxidation, leading to accumulation of inactive {**3,4**} forms of the catalyst.[18–19] Under these conditions, $O_2$ formation becomes rate-limited by (slow) aquation back to the diaqua form of the complex. Because the complex may undergo several cycles of catalysis during its passage through the carbon fiber electrode, particularly at more anodic applied potentials, it is worth considering whether the complexes have been chemically modified by this treatment. Anation is readily detected by cyclic voltammetric experiments, in which large cathodic shifts are observed in $E_{1/2}$ for the {**3,3**}/{**3,4**} wave relative to the active catalyst and waves corresponding to higher oxidations completely disappear.[9] However, in trifluoromethanesulfonic (triflic) acid, voltammograms taken on solutions of electrochemically prepared {**5,5**}, the catalytically active oxidation state, are identical with voltammograms of the starting *cis*,*cis*-diaqua-{**3,3**} complex ion,[16] as originally reported by Meyer's group.[7] Additional studies described in subsequent sections using these solutions to characterize the $\mu$-oxo dimers also gave results equivalent to those of solutions prepared by the titrimetric addition of bolus amounts of the chemical oxidants, $Ce^{4+}$ or $Co^{3+}$.[10,20–22] These results constitute strong evidence that the electrochemically prepared solutions contain unmodified catalyst.
(18) Chronister, C. W.; Binstead, R. A.; Ni, J. F.; Meyer, T. J. *Inorg. Chem.* **1997**, *36*, 3814.
(19) Binstead, R. A.; Chronister, C. W.; Ni, J. F.; Hartshorn, C. M.; Meyer, T. J. *J. Am. Chem. Soc.* **2000**, *122*, 8464.
(20) Lei, Y.; Hurst, J. K. *Inorg. Chem.* **1994**, *33*, 4460.
(21) Lei, Y.; Hurst, J. K. *Inorg. Chim. Acta* **1994**, *226*, 179.
(22) Yamada, H.; Siems, W. F.; Koike, T.; Hurst, J. K. *J. Am. Chem. Soc.* **2004**, *126*, 9786.
(23) Limburg, J.; Vrettos, J. S.; Liable-Sands, L. M.; Rheingold, A. L.; Crabtree, R. H.; Brudvig, G. W. *Science* **1999**, *283*, 1524.
(24) Wada, T.; Tsuge, K.; Tanaka, K. *Inorg. Chem.* **2001**, *40*, 329.
(25) Sens, C.; Romero, I.; Rodriguez, M.; Llobet, A.; Parella, T.; Benet-Buchholz, J. *J. Am. Chem. Soc.* **2004**, *126*, 7798.
(26) Zong, R.; Thummel, R. P. *J. Am. Chem. Soc.* **2005**, *127*, 12802.
(27) Muckerman, J. T.; Fujito, E.; Polyansky, D.; Tanaka, K. *Abstracts of Papers, 233rd National Meeting of the American Chemical Society, Chicago, IL, Mar 25–29, 2007*; American Chemical Society: Washington, DC, 2007.
(28) Yamada, H.; Koike, T.; Hurst, J. K. *J. Am. Chem. Soc.* **2001**, *123*, 12775.
(29) Takeuchi, K. J.; Samuels, G. J.; Gersten, S. W.; Gilbert, J. A.; Meyer, T. J. *J. Am. Chem. Soc.* **2000**, *122*, 8464.
(30) Meyer, T. J. In *Oxygen Complexes and Oxygen Activation by Transition Metals*; Martell, A. E., Sawyer, D. T., Eds.; Plenum Press: New York, 1988; pp 33–48..

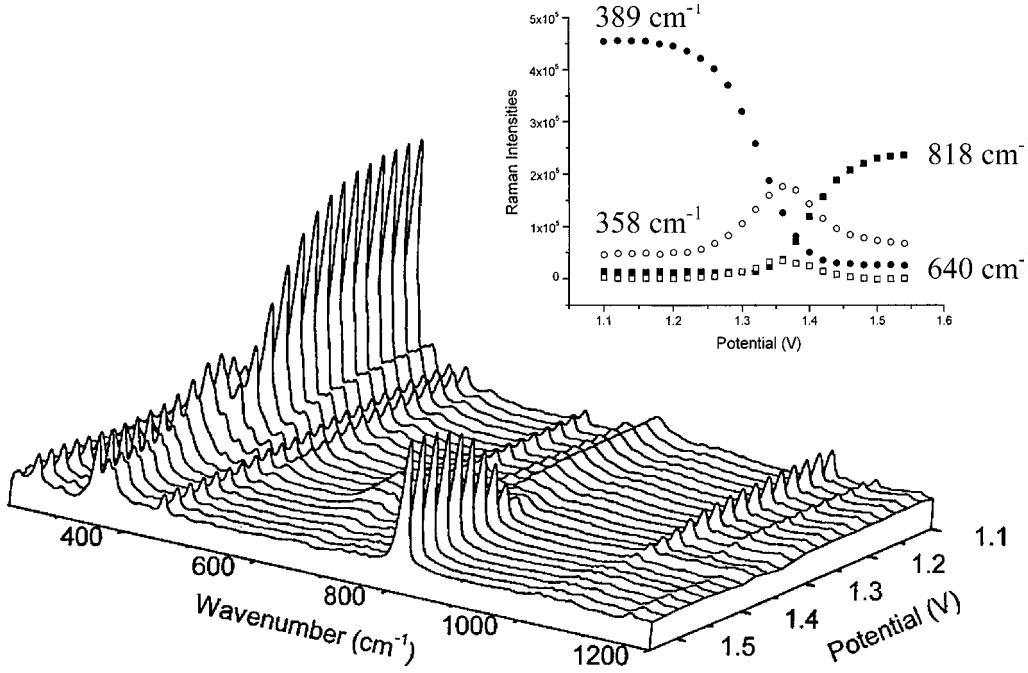


**Figure 3.** RR spectroelectrochemical titration of {**3,4**}. The inset shows selected band intensities plotted as a function of the applied potential.

a {**4,4**} assignment.[16] These differing assignments could be reconcilable if medium conditions influenced the relative thermodynamic stabilities of the ions;[1] in any event, identification of this species may be critical to understanding mechanisms of water oxidation. For this reason, we briefly summarize herein the data supporting a {**4,4**} assignment in aqueous triflic acid. In acidic media, the visible absorption band maximum of {**3,4**} appears at ~444 nm, which is well-resolved from the bands of the higher oxidation states, i.e., ~490 nm for {**4,4**} and ~482 nm for {**5,5**} (Figure 1).[16] Titrimetric addition of 1 equiv of $Ce^{4+}$ causes complete oxidation of {**3,4**} to the intermediate, as determined spectrophotometrically;[28] if the intermediate were {**4,5**}, 2 equiv would have been required. Similarly, mixing equal amounts of {**3,3**} and electrochemically prepared {**5,5**} gave rise to a solution containing just the intermediate;[16] if {**4,5**} were the intermediate, one would have obtained a spectroscopically distinct equimolar mixture of {**3,4**} and {**4,5**}. Solutions of {**5,5**} underwent relatively rapid decay with $O_2$ evolution to the intermediate, which then underwent slow continued decay to the {**3,4**} state; redox titrations with $Os(bpy)_3^{2+}$ (to {**3,3**}) indicate that, at the point at which {**5,5**} disappears from solution, the oxidizing equivalents are reduced to half of their original value,[16] again consistent only with the intermediate being {**4,4**}. In acidic media, {**4,4**} should exist as a dihydroxy complex ion, i.e., $[(bpy)_2Ru^{IV}(OH)]_2O^{4+}$, whereas {**4,5**} should have at least one ruthenyl center, e.g., $(bpy)_2Ru^{IV}(OH)ORu^{V}(O)(bpy)_2^{4+}$; the RR spectrum of the intermediate displays no O-isotope-dependent bands in the 700–900 $cm^{-1}$ spectral region (Figure 3), as expected for {**4,4**} but not {**4,5**}. Additionally, slightly better fits of Nernstian plots to redox spectroelectrochemical titration curves were obtained when the intermediate was assumed to be {**4,4**} rather than {**4,5**}.[16]

**Scheme 1.** Summary of Redox Properties and Stable Oxidation States of *cis,cis*-$[(bpy)_2Ru^{III}(OH_2)]_2O^{4+}$ in 1 M Triflic Acid at 23 °C[a]

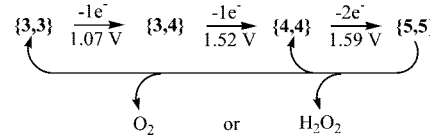


[a] Standard potentials are referenced against NHE. The immediate water oxidation product ($H_2O_2$ or $O_2$) is unknown.

Measurement of decay kinetics in electrochemically prepared {**5,5**} solutions has allowed us to assign {**5,5**} as the $O_2$-evolving species.[22] Specifically, activation parameters for {**5,5**} → {**4,4**} decay are comparable to independently measured values for $O_2$ evolution, whereas the subsequent decay of {**4,4**} is substantially slower (Figure 1). Thus, only {**5,5**} is kinetically competent to be the active catalyst. These conclusions are in accordance with earlier kinetic studies using initial rate methods of $O_2$ evolution from $Ce^{4+}$- or $Co^{3+}$-containing solutions.[16,21] The derived rate laws in those studies were also consistent only with {**5,5**} or a higher oxidation state being the catalytically active form, which underwent unimolecular decay accompanied by $O_2$ evolution. An overall summary of these data is given by the reaction in Scheme 1.

To quantitatively identify the source(s) of O atoms in catalyzed $O_2$ formation, we have developed a reaction cell that allows continuous monitoring of the $O_2$ isotopic composition over the course of 1–2 turnovers of the catalyst (Figure 4).[22] Complexes that contained $^{18}O$-enriched aqua ligands were prepared by water exchange, which is relatively rapid in the {**3,3**} ion ($t_{1/2}$ = 100 s at 23 °C)[28] and then oxidized to {**3,4**} with $Ce^{4+}$, which effectively blocks further water exchange ($t_{1/2}$ > 20 h).[28] Subsequent $O_2$ evolution into the gas phase was monitored via a capillary column connecting the reaction cell to the mass spectrometer; atmo-

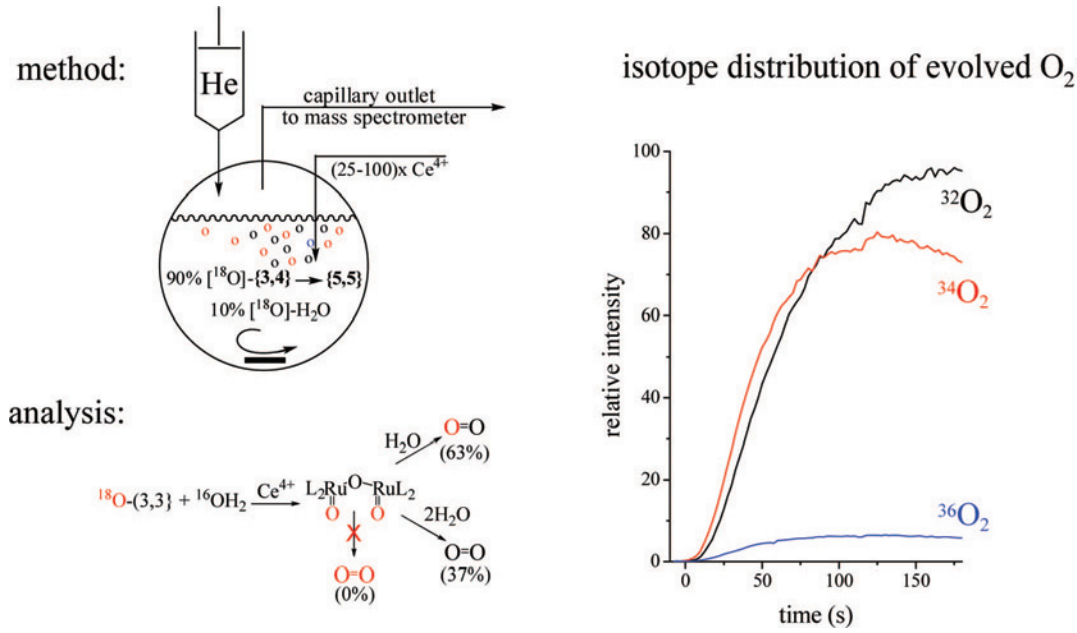


**Figure 4.** Mass spectrometric analysis of the isotopic distribution of O atoms, forming $O_2$ in $\mu$-oxo-dimer-catalyzed water oxidation. Schematic apparatus and typical results for *cis*,*cis*-$[(bpy)_2Ru^V(O)]_2O^{4+}$ in 0.5 M triflic acid.[22]

spheric pressure was maintained by using a syringe as the reservoir for the He carrier gas. By extrapolating the time-dependent data to zero time, one can determine the isotopic composition of the initially formed molecules of $O_2$. Simultaneous monitoring at $m/z = 28$ allows one to accurately correct for adventitious atmospheric $O_2$ and monitoring at $m/z = 44$ allows one to assess the extent of complex degradation (to $CO_2$) accompanying exposure to excess oxidant. In general, only traces of $CO_2$ were formed, and this was observed only in the latter stages of the kinetic runs.

For all of the complexes examined to date (discussed in a succeeding paragraph), two catalyzed pathways for $O_2$ formation have been identified.[31] One pathway entails reaction between a coordinated ruthenyl O atom and solvent $H_2O$ in the critical O−O bond-forming step, while the other involves $O_2$ formation from two solvent molecules. Within experimental uncertainty, no pathway exists for which both O atoms are derived from the complex ions. This unusual result effectively excludes several previously proposed pathways involving unimolecular or bimolecular reductive elimination of $O_2$ from the inner coordination sphere of the complex ions.[22] The relative contributions of the two pathways were found to be independent of the concentrations of catalyst and oxidant but varied with the reaction temperature and identity of the catalyst. For $[(bpy)_2Ru^{III}(OH_2)]_2O^{4+}$, these results are in accordance with previous $^{18}O$-isotope-labeling studies from both Meyer's[32] and our laboratories;[10] because these earlier studies involved periodic bolus sampling of $O_2$ from gaseous headspaces, they provided only qualitative assessment of the major reaction pathways.

## Reaction Mechanisms for the Diruthenium $\mu$-Oxo Ions

Crystallographic structures are available for {**3,3**}[7] and {**3,4**}[33] but not the higher oxidation states. Correspondingly, structures of the various oxidation states of the dimer are being explored through computational analysis. Yang and Baik initially reported that B3LYP density functional theory (DFT) calculations on {**3,3**} indicated that the lowest-energy spin combination is the broken-symmetry antiferromagnetic "weakly coupled" singlet state formed from overlap of the bridging O atom with singly occupied $d_\delta$ orbitals.[34] This result was unanticipated because earlier experimental observations had been interpreted in terms of a strongly coupled antiferromagnetic singlet ground state arising from singly occupied $d_\pi$ orbitals.[35] In a subsequent publication, Yang and Baik reinterpreted their B3LYP calculations to indicate a triplet ground state.[15] Very recent work by Batista and Martin has reinforced this conclusion, although in this case, the singly occupied metal orbitals involved were identified as $d_\pi$.[36] These researchers have also pursued characterization of electronic spin states using complete active space self-consistent-field theory. The lowest-energy state predicted by

(31) This interpretation is valid only if water exchange in the higher oxidation states is slow relative to catalyst turnover. The rates of water exchange cited above were directly measured for the {**3,3**} and {**3,4**} ions by time-dependent determination of their isotopic composition following incubation of $^{18}OH_2$-enriched complexes in water of normal isotopic composition.[28] This was determined from RR spectra obtained following chemical oxidation to {**5,5**} by comparing the intensities of the Ru=$^{16}$O and Ru=$^{18}$O modes. It was also evident from these analyses that water exchange on {**5,5**} was slower than loss of the isotope label from the coordination sphere by catalytic $O_2$ generation. Water exchange on {**4,4**} has not been directly measured, but kinetic simulations clearly indicate that the time course of evolution of the various isotopes (Figure 4) cannot be reproduced by mechanisms that assume rapid exchange of water from any of the higher oxidation states. In contrast, the reaction traces are accurately modeled by the proposed mechanism using independently determined kinetic parameters.

(32) Geselowitz, D.; Meyer, T. J. *Inorg. Chem.* **1990**, *29*, 3894.
(33) Schoonover, J. R.; Ni, J.-F.; Roecker, L.; White, P. S.; Meyer, T. J. *Inorg. Chem.* **1996**, *35*, 5885.
(34) Yang, X.; Baik, M.-H. *J. Am. Chem. Soc.* **2004**, *126*, 13222.
(35) Weaver, T. R.; Meyer, T. J.; Adeyemi, S. A.; Brown, G. M.; Eckberg, R. P.; Hatfield, W. E.; Johnson, E. C.; Murray, R. W.; Untereker, D. *J. Am. Chem. Soc.* **1975**, *97*, 3039.
(36) Batista, E. R.; Martin, R. L. *J. Am. Chem. Soc.* **2007**, *129*, 7224.

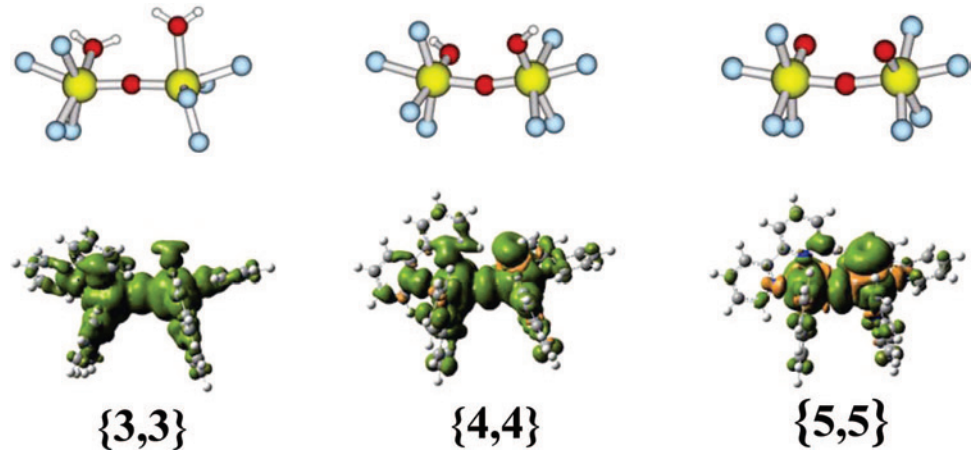


**Figure 5.** B3LYP/6-31G*/LANL2DZ high-spin ferromagnetically coupled optimized conformations of the $\{\mathbf{3,3}\}^{4+}$, $\{\mathbf{4,4}\}^{4+}$, and $\{\mathbf{5,5}\}^{4+}$ ions. Plots of the spin densities for each oxidation state, at an isovalue of 0.004, are shown below.

these calculations is a weakly antiferromagnetically coupled broken-symmetry singlet state with 80% localization of the unpaired spin density.[36] We have also become interested in the electronic spin states of the dimer. The structures for high-spin ferromagnetically coupled {**3,3**}, {**4,4**}, and {**5,5**} predicted from DFT calculations (B3LYP/LANL2dz/6-31G*) are shown in Figure 5. A complete description of the computed higher spin coupled states including mixed-valent ions and low-spin electronic states will appear in a forthcoming paper. However, the following results are pertinent to this discussion: the energy-minimized structure for {**3,3**} is very similar to the published X-ray structure, although core bond lengths are ~0.1 Å longer in the computed structure; oxidation to {**4,4**} and {**5,5**} is accompanied by only minimal changes in structure, comprising slight contraction of the bond lengths and a small increase in the O−Ru−Ru−O dihedral angle defined by the metals and terminal O atoms; the calculated values for $\nu_{sym}$(Ru−O−Ru) are lower than the experimental values by 50–100 $cm^{-1}$, consistent with the longer predicted bond lengths; $\nu_{sym}$(Ru−O−Ru) does not change appreciably upon oxidation, consistent with experimental results (Figure 3) that indicate nearly constant bond lengths in a nearly linear Ru−O−Ru bridge; unpaired spin densities also remain relatively constant within the$[Ru(O)]_2O$ core upon progressive oxidation, with loss of the electron spin density appearing primarily in the bipyridine ligands (Figure 5); the calculated barrier to free rotation about the Ru−O−Ru bond is ~15 kcal/mol. These results describe a relatively rigid complex whose terminal O atoms are separated by ~4.5 Å. Intramolecular reductive elimination of $O_2$ is therefore expected to be energetically unfavorable, consistent with the isotope-labeling results.

To account for the pathway involving $O_2$ formation from one ruthenyl O atom and one molecule of solvent, we have proposed a mechanism initiated by concerted addition of the elements of $H_2O$ across the $[Ru(O)]_2O$ core of the {**5,5**} ion (Scheme 2).[22]

In this reaction, homolytic cleavage of the solvent O−H bond, assisted by H-atom abstraction at one ruthenyl center, is accompanied by O−O bond formation between the incipient OH fragment and the other ruthenyl O atom. The

**Scheme 2.** Pathway for the Concerted Addition of $H_2O$ across the {**5,5**} $[Ru(O)]_2O$ Core, Leading to $O_2$ Formation from One Solvent Molecule and One Ruthenyl O Atom[a]

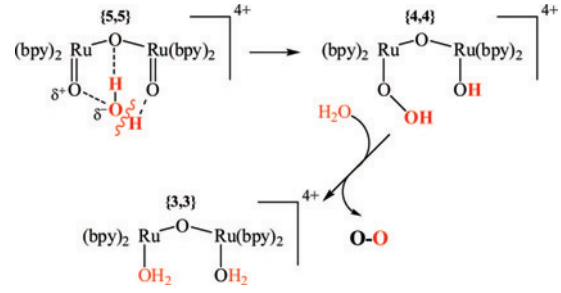


[a] The atoms highlighted in red are from noncoordinated $H_2O$.

concerted nature of the process avoids formation of high-energy intermediates, e.g., free OH•, or contributions to activation barriers arising from extensive structural alterations within the complexes, i.e., changes in the coordination number or overall electrostatic charges. The immediate reaction products obtained from the reaction of the peroxo-bound intermediate are unknown, but a likely decay channel is intramolecular electronic rearrangement to give {**3,3**} and $O_2$. Loss of $O_2$ from the inner coordination sphere of a ruthenium would generate an intermediate with a reduced coordination number, however, which becomes susceptible to inactivation by competitive anation at that site.[18,19] The mechanism of O−O bond formation is consistent with general reactivity principles established for other ruthenyl compounds. Specifically, kinetic studies of oxidation of O−H and C−H bonds in a variety of organic and inorganic compounds catalyzed by monomeric ruthenyl complexes have revealed unusually large kinetic isotope effects, which have been attributed to rate-limiting H-atom abstraction to the ruthenyl O atom.[37] Additionally, a detailed DFT study of potential reaction profiles has been conducted, which provides theoretical support for this mechanism.[15] The only low-energy pathway found in that computational study was

(37) (a) Gilbert, J.; Roecker, L.; Meyer, T. J. *Inorg. Chem.* **1987**, *26*, 1126. (b) Roecker, L.; Meyer, T. J. *J. Am. Chem. Soc.* **1987**, *109*, 746. (c) Mayer, J. M. *Acc. Chem. Res.* **1998**, *31*, 441. (d) Bryant, J. R.; Mayer, J. M. *J. Am. Chem. Soc.* **2003**, *125*, 10351.

**Scheme 3.** Pathway for $O_2$ Formation from Two Solvent Molecules Based upon the Formation of a Bridging Ozonide Ligand

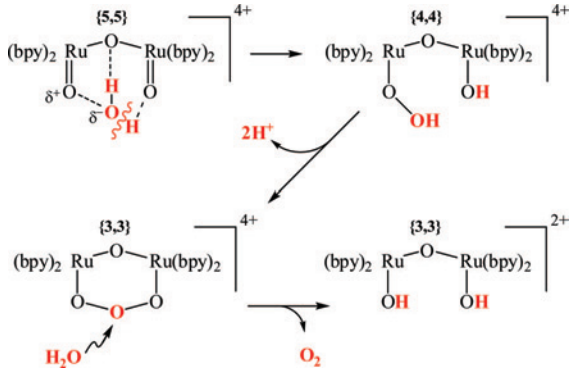


one analogous to that given in Scheme 2; the calculated overall activation barrier was 26 kcal/mol, which is close to the experimental values obtained for $O_2$ evolution ($\Delta G^{\ddagger} \approx$ 20 kcal/mol in 0.5 M triflic acid, 23 °C).

Devising a plausible reaction mechanism for the other pathway, in which both O atoms are obtained from solvent, is considerably more problematic. One inventive mechanism suggested by Meyer is that a mixed dibridged intermediate containing an ozonide group is formed that undergoes attack at the central O atom by $H_2O$ to generate $O_2$.[30] An intermediate of this type might form, e.g., by rearrangement of the hydroperoxy−hydroxy intermediate formed by water addition to the {**5,5**} core (Scheme 3).

However, thermodynamic considerations based upon more recent estimates of $\Delta H_f°$ for $H_2O_3$ suggest that collapse of a peroxo precursor to an ozonide intermediate would be energetically prohibitive.[22,38] Alternative mechanisms that might be entertained involve either expansion of the ruthenium coordination sphere by the addition of a solvent or "noninnocent" participation of bipyridine ligands. One cannot consider distinguishing between these possibilities without becoming immersed in broader issues concerning the reactivities of ruthenium complexes that were raised long ago yet have remained largely unresolved.[39]

Nonetheless, our recent experiments have been designed primarily to test the notion that the bipyridine ligands participate in catalysis. A hypothetical mechanism illustrating how this might occur is given in Scheme 4.[22] As before, the reaction is initiated by concerted addition of the elements of $H_2O$ to the complex ion; however, in this case, the incipient OH fragment adds to the bipyridine ring, rather than the second ruthenyl O atom, giving rise to a ligand radical coordinated to {**4,5**}. The addition of a second $H_2O$ molecule to the ring would generate a {**4,4**}-diol whose ruthenium core is nearly as strong of a two-electron oxidant as the original {**5,5**} ion (Scheme 1). Ligand oxidation to form a {**3,3**}-endoperoxide, followed by electronic rearrangement[40] eliminating $O_2$, would regenerate {**3,3**}, completing the catalytic cycle. As in the other mechanism, the overall electrostatic charge is unchanged through the cycle, thereby avoiding potentially large contributions from this source to activation barriers for individual steps. Presumably, the presence of a two-electron sink (represented by {**4,4**}) reduces the lifetime of diol intermediates, lowering the susceptibility of the bipyridine ring toward hydrolytic degradation. One should note that placement of OH groups in the scheme is arbitrary; the addition to the N atom or bridging C atom would give intermediates that are expected to be less susceptible to oxidative degradation.

**Scheme 4.** Pathway for $O_2$ Formation from Two Solvent Molecules Based upon Covalent Hydration of a Bipyridine Ligand

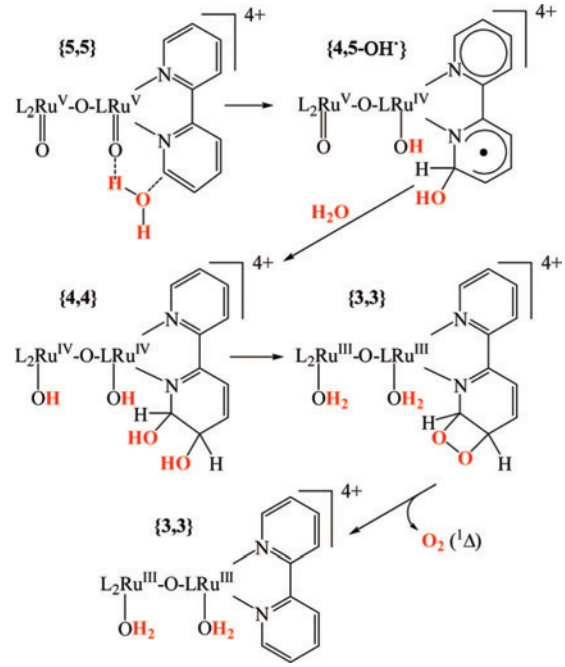


The notion that ruthenium diimine complexes can add $H_2O$ to their ligands has its origin in extensive studies on "covalent hydration" of several classes of nitrogen heteraromatic compounds conducted in the 1960s.[41] A simple example of the phenomenon is the hydration of pteridine shown below. In aqueous solution, the pteridine neutral base is ~80% in the anhydrous form shown here; protonation activates the molecule for the addition of $H_2O$ across a second N=C bond, so that at equilibrium the conjugate acid is nearly completely hydrated. In general, two major factors that promote covalent hydration in these compounds are electron withdrawal from the heterocyclic ring and resonance stabilization of the hydrated form, i.e., the resonance forms shown in brackets. By analogy with these reactions, inductive withdrawal of the electron density from the bipyridine rings by the coordinated $Ru^V$ center (Figure 5) could promote water addition. Heterocycles containing two added $H_2O$ molecules also exist,[41] giving credence to the postulated formation of {**4,4**}-diol intermediates of the type shown in Scheme 4.

The following experimental results obtained in our laboratory, although not definitive, appear consistent with the

(38) Lay, T. H.; Bozzelli, J. W. *J. Phys. Chem. A* **1997**, *101*, 9505.
(39) (a) Gillard, R. D. *Coord. Chem. Rev.* **1975**, *16*, 67. (b) Serpone, N.; Ponterini, G.; Jamieson, M. A.; Bolletta, F.; Maestri, M. *Coord. Chem. Rev.* **1983**, *50*, 209. (c) Gillard, R. D. *Coord. Chem. Rev.* **1983**, *50*, 303.
(40) Wasserman, H. H.; Scheffer, J. R. *J. Am. Chem. Soc.* **1967**, *89*, 3073.
(41) (a) Albert, A.; Armarego, W. L. F. *Adv. Heterocycl. Chem.* **1965**, *4*, 1. (b) Albert, A. *Adv. Heterocycl. Chem.* **1976**, *20*, 117.

proposed mechanism.

(1) Introducing electron-donating substituents on the

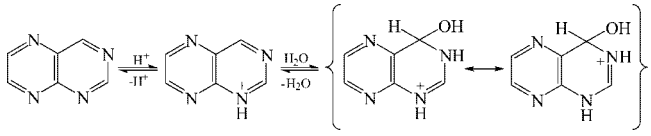

bipyridine ring should both sterically and electronically hinder adduct formation with water, thereby restricting this reaction; conversely, electron-withdrawing substituents might promote adduct formation if electronic factors are dominant.[41] Preliminary results on the relative contributions of the two pathways determined by $^{18}O$-isotope-labeling studies for several substituted bipyridine-substituted catalysts are presented in Figure 6. The data indicate that the relative contribution of this pathway increases progressively in parallel with the electron-withdrawing character of the substituent group, consistent with the proposed mechanism.

(2) A hydroxyl radical has been shown to add to the bipyridine ring in the free ligand and several group 8 $M(bpy)_3^{n+}$ complex ions, giving rise to intermediates that possess characteristic weak optical bands in the 750–800 nm region.[3] This behavior is consistent with the well-known preference of OH$^\bullet$ to form covalent adducts with aromatic and heterocyclic compounds rather than undergo one-electron reduction to a hydroxide ion. As illustrated in Figure 7 for {**3,3**}, comparable reactions are observed for the "blue" dimer in either of its stable oxidation states when exposed to radiolytically generated OH$^\bullet$. Here, a loss of intensity in the blue band (640 nm) coincides with the formation of a new near-IR band (780 nm), which subsequently undergoes unimolecular decay with the formation of species absorbing at ~490 nm. Our proposed mechanism (Figure 7) involves internal electron transfer from the initial bpy-OH$^\bullet$ adduct to a ruthenium center, generating initially {**2,3**}-bpyOH, the Ru−O−Ru bond of which is unstable and rapidly hydrolyzes to give monomeric $Ru^{II}$ and $Ru^{III}$ complexes.[7] Comparable internal electron transfer following OH$^\bullet$ adduct formation has previously been observed for other coordination complexes containing aromatic ligands.[42] Adduct formation between

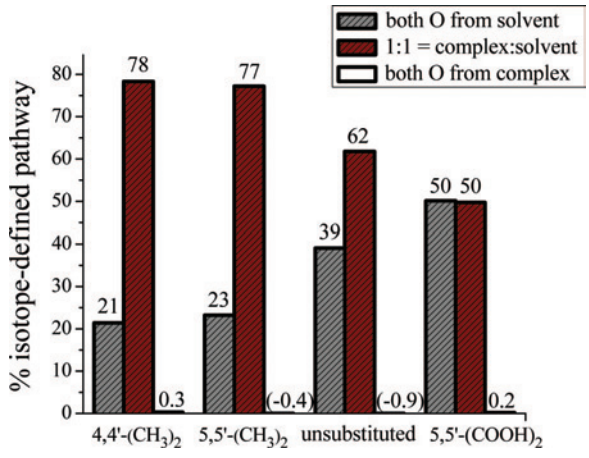


**Figure 6.** Influence of bipyridine substituents upon pathway distributions. The numbers over the bars are the percentage reaction by an isotope-defined pathway.

OH$^\bullet$ and the "blue" dimer supports the plausibility of similar OH addition to the ring in reactions of {**5,5**} with $H_2O$. Moreover, we have now observed a very similar band at ~750 nm that appears during $O_2$-evolving photosensitized reactions involving the water oxidation catalyst. These reactions are analogous to a system previously reported from the Grätzel laboratory[9] involving $S_2O_8^{2-}$ oxidation of a photoexcited $Ru(bpy)_3^{2+}$ derivative to $Ru(bpy)_3^{3+}$ followed by cyclic rereduction to $Ru(bpy)_3^{2+}$ by {**3,3**} and higher oxidation states of the dimer, leading to eventual formation of the $O_2$-evolving oxidation state (Figure 8). Temporal changes in optical spectra of the solutions under continuous illumination require inclusion of a near-IR band (Figure 8), the intensity of which is proportional to the catalyst concentration and $O_2$ evolution rate but independent of the photosensitizer concentration. The cumulative results suggest that the near-IR band is attributable to an active intermediate containing an OH-bipyridine adduct and not merely a side product developing during the photoredox reactions. Tanaka and associates have also suggested that quinine−semiquinone redox cycling of benzoquinone ligands is essential to catalytic function in the novel diruthenium water oxidation catalyst that they have developed.[24,27]

(3) Cryogenic EPR signals are detected in samples of {**5,5**} prepared in acidic media by either chemical[20] or potentiometric oxidation[16] of {**3,3**} that are quite unlike the broad rhombic signals usually observed for ruthenium-centered paramagnetic ions (Figure 9). The intensities of these signals are proportional to the {**5,5**} concentration but represent only ~10% of the expected spin density, indicating that they constitute only a minor component of the solutions. Apparent six-line hyperfine splitting is observed for ~25% of the signal, which can be provisionally assigned to coupling to single $^{99}Ru$ and $^{101}Ru$ nuclei, isotopes for which $I_N = {}^5/_2$ and which collectively are in 30% natural abundance. Although characterization of these signals is incomplete, they appear to have properties expected of ligand radical reaction intermediates such as {**4,5**}-bpyOH$^\bullet$ (Scheme 4), i.e., a relatively narrow axially symmetric $g \sim 2$ signal. Notably, very similar EPR signals have recently been reported for a monomeric organometallic ruthenium complex, $[(\eta^5\text{-}C_5Me_5)RuCl_2(S_2CNME_2)]^+$,[43] which is formally $Ru^V$, although DFT calculations indicate that its chlorine ligands are highly electron-deficient.

The mechanism given in Scheme 4 is by no means unique. Very similar bipyridine-OH adducts have been proposed to account for $O_2$ generation during alkaline decomposition of group 8 $M(bpy)_3^{3+}$ ions,[3,4] and complexes containing dihydroxy-substituted bipyridines analogous to {**4,4**}-diol have been suggested as intermediates in the irreversible degradation of the ligand.[2] The different outcome observed for the dimeric ruthenium catalysts may reflect the presence of a two-electron sink in the form of the $Ru^{IV}$−O−$Ru^{IV}$ core; as previously noted, the addition of redox-active $Co^{2+}$ to the

(42) Hoffman, M. Z.; Kimmel, D. W.; Simic, M. G. *Inorg. Chem.* **1979**, *18*, 2479.
(43) Kuan, S. L.; Tay, E. P. L.; Leong, W. K.; Goh, L. Y.; Lin, C. Y.; Gill, P. M. W.; Webster, R. D. *Organometallics* **2006**, *25*, 6134.

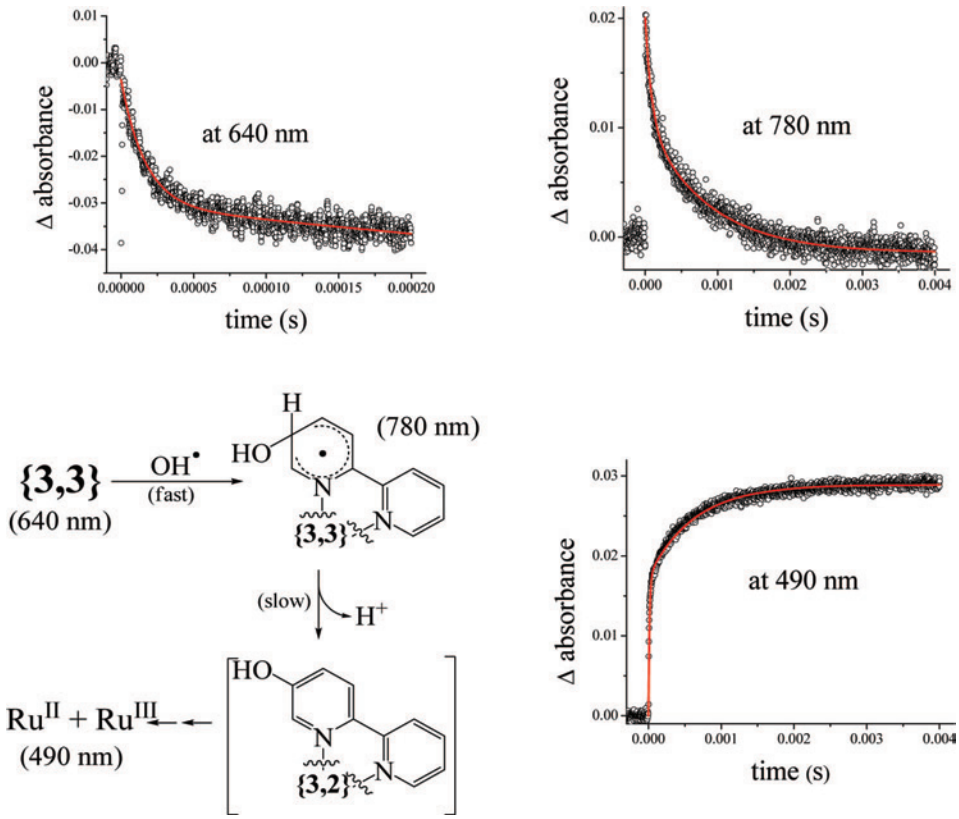


**Figure 7.** Reaction of {**3,3**} with pulse radiolytically generated OH•. Kinetic traces taken at various wavelengths are displayed with their mechanistic interpretation presented in the accompanying scheme (lower left). Conditions: 50 $\mu$M catalyst in $N_2O$-saturated 0.1 M potassium triflate, 5 mM potassium phosphate, pH 5, at 23 °C.

$Ru(bpy)_3^{3+}$ solutions protected them from ligand decomposition while promoting $O_2$ formation.[2,5] In their study of reactions of zeolite-encaged $Ru(bpy)_3^{3+}$ with $OH^-$, which were reported to give near-quantitative yields of $O_2$, Ledney and Dutta also found evidence for the accumulation of reaction transients in the 700–800 nm region and of relatively sharp $g \sim 2$ EPR signals, which they attributed to ligand-centered radicals.[4] Their proposed mechanism also invoked the formation of covalent hydrates and pseudobase adducts with bipyridine ligands. More recently, Thummel's laboratory has reported that dinuclear ruthenium complexes formed within chelating bis(napthyridylpyridyl)pyridazine scaffolds are also capable of catalyzing water oxidation by strong oxidants despite having no coordinated aqua ligands.[26] Thus, there are now several examples of homogeneous catalysis of $O_2$ generation solely from solvent molecules, suggesting that participation of N-heterocyclic ligands could be quite general and potentially exploitable for the development of new catalysts.

### Catalytic Activity of the $\mu$-Oxo Dimers

Most kinetic studies on the catalyzed reaction have been made in strongly acidic solutions. Under these conditions, the turnover rate constant for $O_2$ formation is $k_{cat} \approx 10^{-2}$ $s^{-1}$,[21,22] which is at least $10^4$-fold slower than water oxidation by the $O_2$-evolving complex (OEC) of photosystem II.[44] However, the photosensitized reaction rate increases progressively with increasing alkalization to pH ~9, where the apparent rate constant for $O_2$ formation maximizes at $k_{cat} \sim 2\ s^{-1}$, based upon the total amount of catalyst present (Figure 10). The distribution of catalyst oxidation states under continuous photolysis has not yet been determined; however, the steady-state ratio of photosensitizer oxidation states estimated by component spectral fitting (Figure 8) indicates that oxidation of {**3,4**} to {**4,4**} is incomplete and therefore that {**5,5**} is a minor fraction of the total complex ion present in the steady state. Assuming that {**5,5**} is also the sole $O_2$-evolving species under these conditions, the actual turnover rate constant could easily be an order of magnitude larger, e.g., $k_{cat}\{\mathbf{5,5}\} \approx 20\ s^{-1}$, comparable to the best values reported for metal oxide catalysts[6] and approaching the rate constant for biological water oxidation by the OEC.[41] Optimized quantum yields ($\Phi$) for the photosensitized systems (Figure 10), defined as $O_2$ formed/quantum absorbed by the photosensitizer, are typically $\Phi \sim 0.2$, which is also encouraging. These values can be compared to a theoretical yield of $\Phi = 0.25$–$0.5$ (the range arising because the fate of $SO_4^{\bullet -}$ formed upon oxidative quenching of photoexcited $Ru(bpy)_3^{2+}$ by $S_2O_8^{2-}$ is uncertain). Thus, there is reason to believe that the continued development of multinuclear coordination complexes of this general class will lead to homogeneous catalysts with performance characteristics that rival biological water oxidation.

(44) Clausen, J.; Debus, R. J.; Junge, W. *Biochim. Biophys. Acta* **2004**, *1655*, 184.

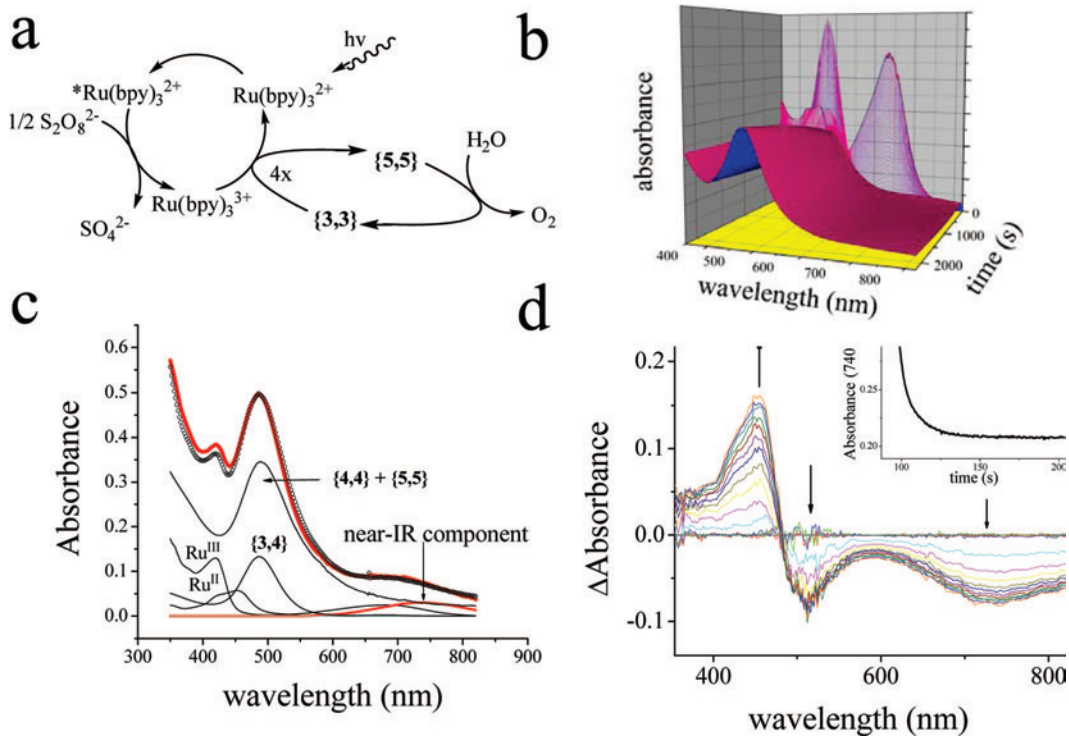


**Figure 8.** Photosensitized water oxidation catalyzed by {**3,3**}: (a) proposed mechanism; (b) time-resolved absorbance spectrum for a reaction containing 60 $\mu$M $Ru(bpy)_3^{2+}$, 60 $\mu$M {**3,3**}, and 5 mM $K_2S_2O_8$ in 0.1 M phosphate, pH 7.2; (c) concentrations of species in the steady state determined by fitting of the experimental spectrum to spectra for redox components involved in the reaction cycle [{**3,3**}, {**3,4**}, {**4,4**} + {**5,5**}, $Ru(bpy)_3^{2+}$, and $Ru(bpy)_3^{3+}$] and a previously unidentified near-IR component centered at 740 nm; (d) difference absorption spectra of transient decay during a light-to-dark transition in the continuous photolysis reaction, showing conversion of {**4,4**} + {**5,5**} to {**3,4**} and the decay of the near-IR component (inset).

## Future Directions toward Redox-Driven Solar Photoconversion

There are several daunting technological obstacles to utilizing multinuclear coordination complexes as catalysts in water oxidation half-cycles for solar-driven energy production and utilization. Perhaps the most significant are the absence of any efficient catalysts based upon the relatively abundant first-row transition elements, the often rapid loss of catalytic activity during turnover (presumably by irreversible degradation of reactive intermediates), and the virtual absence of intrinsic photoredox activity that might be used to harvest solar energy and/or drive the reductive half-cycles. These are in addition to more general constraints that seemingly require some form of compartmentalization of the half-cycles to minimize energy-dissipating cross-reactions between reactants, intermediates, and products. Compartmentalization, in turn, leads to a further set of issues (which are not frequently discussed) relating to avoidance or dissipation of intercompartmental electrochemical gradients generated by charge transport.[45]

The extensive efforts[46] directed at developing manganese-based catalysts by mimicking perceived structures of the $Mn_4$ center in the OEC or $Mn_2$ centers in other redox enzymes have not yet met with much success. The few dinuclear complexes that are reported to exhibit water-oxidizing capability[23,47] bear little structural relationship to the OEC;[48] the most extensively studied of these, $[(terp)_2Mn_2^{III/IV}(\mu\text{-}O)_2(H_2O)_2]^{3+}$,[23] is structurally much more closely related to the "blue" dimer. In direct comparisons, however, the

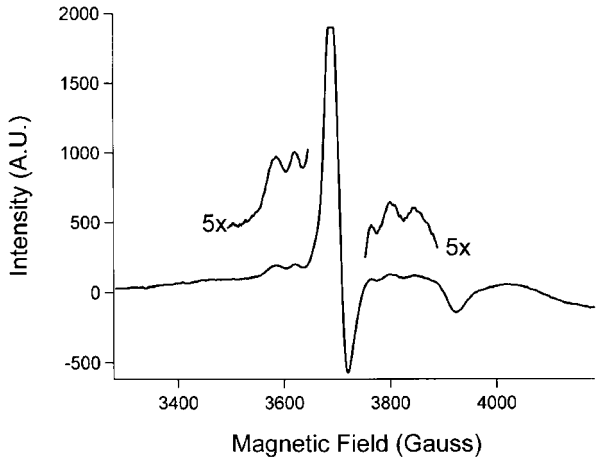


**Figure 9.** X-band EPR spectrum of {**5,5**} at ~10 K.[1,16,20]

(45) Hurst, J. K.; Khairutdinov, R. F. In *Electron Transfer in Chemistry*; Balzani, V., Ed.; Wiley-VCH: Weinheim, Germany, 2000; Vol. *4*, pp 578–623..

(46) (a) Christou, G.; Vincent, J. B. *ACS Symp. Ser.* **1987**, *372*, 238. (b) Wieghardt, K. *Angew. Chem., Int. Ed. Engl.* **1989**, *28*, 1153. (c) Andreasson, L.-E.; Vanngard, T. In *Encyclopedia of Inorganic Chemistry*; King, R. B., Ed.; Wiley: New York, 1994; Vol. *4*, p 2102. (d) Ruttinger, W.; Dismukes, C. *Chem. Rev.* **1997**, *97*, 1. (e) Mukhopadhyay, S.; Mandal, S. K.; Bhaduri, S.; Armstrong, W. H. *Chem. Rev.* **2004**, *104*, 3981.

(47) (a) Naruta, Y.; Sasyama, M.; Sasaki, T. *Angew. Chem., Int. Ed. Engl.* **1994**, *33*, 1839. (b) Poulsen, A. K.; Rompel, A.; McKenzie, C. J. *Angew. Chem., Int. Ed. Engl.* **2005**, *44*, 6916. (c) Narita, K.; Kuwabara, T.; Sone, K.; Shimizu, K.; Yaga, M. *J. Phys. Chem. B* **2006**, *110*, 23107.

(48) Yano, J.; Kern, J.; Sauer, K.; Latimer, M. J.; Pushkar, Y.; Biesiadka, J.; Loll, B.; Saenger, W.; Messinger, J.; Zouni, A.; Yachandra, V. *Science* **2006**, *314*, 821.

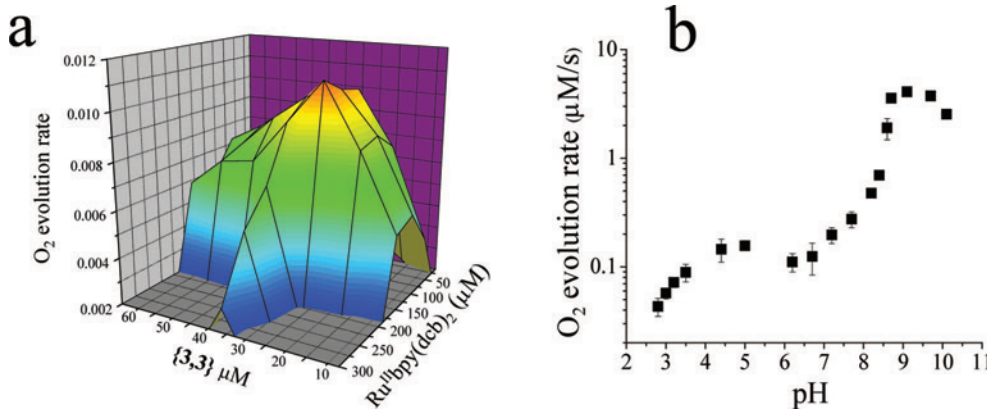


**Figure 10.** Dependence of $O_2$ evolution rates in photosensistized reactions upon reaction parameters: (a) {**3,3**} and sensitizer (S) concentration dependencies at pH 7.2 and an incident flux of $6 \times 10^{-8}$ einstein/s [S = $Ru(dcb)_2(bpy)^{2+}$; dcb = 4,4′-dicarboxy-2,2′-bipyridine]; (b) pH dependence at 30 $\mu$M {**3,3**} plus 50 $\mu$M $Ru(bpy)_3^{2+}$ and an incident flux = $4 \times 10^{-8}$ einstein/s. All reactions at 23 °C in 0.1 M phosphate containing 5 mM $K_2S_2O_8$.

manganese dimer has not been nearly as active of a catalyst as {**3,3**}; for example, we find that the manganese dimer is not capable of supporting $O_2$ generation in the photocatalytic system described in Figure 8. Although the redox cycling of {**3,3**} (Scheme 1) is superficially similar to the Kok cycles written for the OEC,[49] i.e., four sequential one-electron oxidations accompanied by proton loss, the mechanisms of water oxidation that we propose (Schemes 2 and 4) are unlike the mechanisms currently invoked for biological water oxidation,[50] which feature nucleophilic attack of a coordinated $H_2O$ molecule at a single manganyl O atom in the O−O bond-forming step. While not wishing to dissuade researchers in their efforts to model the OEC, particularly now that accurate structures of that center are forthcoming,[48] it would seem prudent to spend equivalent effort in exploring iron-based complexes as potential water oxidation catalysts, particularly because the early literature suggests that the relevant redox behavior of $Fe(bpy)_3^{3+}$ may parallel that of $Ru(bpy)_3^{3+}$.[1] Individuals seeking to be "bioinspired" might find it productive to look carefully at redox enzymes such as methane monooxygenase, whose di($\mu$-oxo)diiron center has been suggested to function via radicaloid electronic states reminiscent of the one calculated for {**5,5**}.[51]

Several approaches can be considered for improving the catalytic effectiveness of transition-metal ions as water oxidation catalysts, with respect to both longevity and photocatalyst development. "Deactivation" of ligands toward covalent hydration or pseudobase formation by appropriate derivatization or synthesis of new multidentate scaffolding ligands of the type recently devised by Thummel and coworkers[26] that, however, retain the$[M(O)]_2O$ core could serve to minimize the formation of unstable ligand radical species that lead to degradative side reactions. Based upon Ledney and Dutta's remarkable observation that decomposition of $Ru(bpy)_3^{3+}$ during catalyzed $O_2$ evolution was blocked by zeolite encapsulation,[4] synthesis of more elaborate encapsulating or dendrimeric ligands might be used to hinder bimolecular decomposition pathways. Adsorption or covalent attachment to particulate surfaces could accomplish the same objective. The ruthenium-based water oxidation catalysts exhibit only very modest photoactivation toward water oxidation. Photoactivation could be achieved by introducing photosensitizers capable of oxidatively quenching the catalyst, e.g., in place of the unstable $S_2O_8^{2-}Ru(bpy)_3^{2+}$ photooxidation system shown in Figure 8. To improve photoefficiencies, these sensitizers might be covalently linked to the oxidation catalyst to form sensitizer−donor dyads or more highly organized electron-transport assemblies. This strategy is being actively pursued in several laboratories; our own recent efforts have been directed at coupling $[L_2Ru^{III}(OH_2)]_2O^{4+}$-catalyzed water oxidation to transmembrane charge separation across ion-impermeable bilayer membranes. The central components of these organized assemblies are pyrylium ions, which can function when photoexcited with visible light as combined photosensitizers for catalyst-mediated water oxidation and electroneutral transmembrane $e^-/OH^-$ antiporters.[52] The entire assemblies constitute compartmented systems on the mesoscopic scale for separation of the reaction half-cycles for photoinduced water splitting; the actual transmembrane redox carriers are uncharged, obviating the need to address issues associated with membrane polarization.

Necessity alone will drive growth in this area of endeavor. Fortunately, the field seems poised for rapid advance. The "blue" dimers exhibit considerably higher catalytic activity than has been previously recognized, efficient particulate metal ion and metal oxide based (e.g., $IrO_2$)[6] catalysts are also being developed, increasing attention is being given to integrating water oxidation catalysts into photocatalytic systems (where they may function more effectively), and new avenues for synthesis of more durable catalysts are being developed,[24,26] as are theoretical methods to address mechanistic issues and provide direction for improved catalyst design. Although there is much to be done and time may be short, there is also reason for optimism that the seemingly large technological hurdles impeding the development of practical catalytic systems can be overcome.

(49) Kok, B.; Forbush, B.; McGloin, M. *Photochem. Photobiol.* **1970**, *11*, 457.
(50) McEvoy, J. P.; Brudvig, G. W. *Chem. Rev.* **2006**, *106*, 4455.
(51) Baik, M.-H.; Gherman, B. F.; Friesner, R. A.; Lippard, S. J. *J. Am. Chem. Soc.* **2003**, *124*, 14608.
(52) Khairutdinov, R. F.; Hurst, J. K. *J. Am. Chem. Soc.* **2001**, *123*, 7352.

**Acknowledgment.** J.K.H. is grateful for the long-standing financial support of the Office of Basic Energy Sciences, U.S. Department of Energy (Grant 06ER15820), and for the dedicated efforts of former students and research associates, whose accomplishments have laid the foundation for our ongoing studies. Prominent among these individuals are Hiroshi Yamada, Rafail F. Khairutdinov, Linyong Zhu, Yabin Lei, Jinzhong Zhou, and Sergei V. Lymar (with whom collaboration is continuing at Brookhaven National Laboratory).

IC700724H